

## Accepted Manuscript

### Natural Convection Effects in Electrochemical Systems

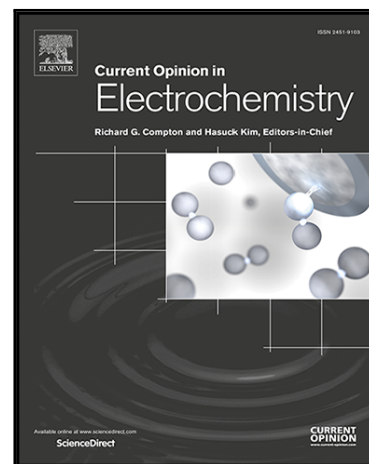
Javor K. Novev , Richard G. Compton

PII: S2451-9103(17)30125-4  
DOI: [10.1016/j.coelec.2017.09.010](https://doi.org/10.1016/j.coelec.2017.09.010)  
Reference: COELEC 111

To appear in: *Current Opinion in Electrochemistry*

Received date: 16 August 2017  
Accepted date: 19 September 2017

Please cite this article as: Javor K. Novev , Richard G. Compton , Natural Convection Effects in Electrochemical Systems, *Current Opinion in Electrochemistry* (2017), doi: [10.1016/j.coelec.2017.09.010](https://doi.org/10.1016/j.coelec.2017.09.010)



This is a PDF file of an unedited manuscript that has been accepted for publication. As a service to our customers we are providing this early version of the manuscript. The manuscript will undergo copyediting, typesetting, and review of the resulting proof before it is published in its final form. Please note that during the production process errors may be discovered which could affect the content, and all legal disclaimers that apply to the journal pertain.

**Highlights**

- Recent work on natural convection in electrochemistry is reviewed.
- Experimental and theoretical/simulation studies in the area are considered.
- Free convection driven by concentration and/or temperature gradients is discussed.
- Natural convection in systems such as electrorefining and fuel cells is covered.
- A critical assessment of the concept of 'spontaneous convection' is given.

ACCEPTED MANUSCRIPT

# Natural Convection Effects in Electrochemical Systems

Javor K. Novev and Richard G. Compton\*

Department of Chemistry, Physical and Theoretical Chemistry Laboratory, Oxford  
University, South Parks Road, Oxford, OX1 3QZ, UK.

\*Corresponding author. E-mail: [Richard.Compton@chem.ox.ac.uk](mailto:Richard.Compton@chem.ox.ac.uk); Fax: +44 (0)1865 275 410; Tel: +44 (0)1865 275 957

## Keywords

natural convection, thermal convection, solute-driven convection, transport phenomena, electrochemical simulations, 'spontaneous convection'

**Abstract:** Natural (free) convection influences electrochemical processes that occur in areas as disparate as electroanalytical sensing and copper electrorefining. The modelling of natural convection requires solving a set of coupled partial differential equations reflecting the interplay between the transport of mass, heat and momentum that lies at the core of this phenomenon. This article reviews recent developments in the study of the subject, and covers various cases, e.g. free convection driven by concentration and/or temperature gradients, bubble-induced convection, and natural convection coupled with an external force. Literature on free convective flows in practical contexts such as fuel and thermogalvanic cells and electrochemical sensors is also discussed. Recent articles that describe experimental approaches for minimizing the effect of natural convection are covered. Studies which take advantage of the analogy between mass and heat transfer in order to probe the latter are discussed in brief. Particular attention is devoted to a critical assessment of the concept of 'spontaneous convection', which has been invoked in a number of recent papers.

## 1. Introduction

*Natural (free) convective flows* arise within fluids of spatially inhomogeneous density subjected to the force of gravity and can influence both mass and heat transport [1]. The fluid motion affects the total flux of a solute ('i') [2],

$$\mathbf{J}_i = -D_i \nabla C_i - \frac{D_i C_i z_i F}{RT} \nabla \phi + C_i \mathbf{v}, \quad (1)$$

where  $D_i$  is the diffusivity of the species,  $C_i$  – its concentration,  $z_i$  – its charge,  $\phi$  is the electrical potential in the solution, and  $R$  and  $F$  are respectively the gas and Faraday constants. In the absence of an external factor driving fluid motion (i.e., *forced* convection), the velocity  $\mathbf{v}$  is determined by natural convection. As insightfully and authoritatively remarked by Levich [1], there are two factors that may induce natural convection:

*Motion of the solution in natural convection is spontaneous and arises due to forces originating from heterogeneous reactions. Such forces usually follow the changes in the density of the solution which accompany the reaction. . . . Changes in the density of the solution may be caused by two phenomena: first, the concentration in the proximity of the reaction surface changes in the course of a heterogeneous reaction and leads to changes in the density of the solution; second, if the heterogeneous reaction is exothermic and is accompanied by a substantial release of heat, the density of the solution changes from point to point as a result of non-uniform changes in the temperature of the solution. . . .*

*Natural convection arises only when the density change occurs in the gravitational field, and only in those cases where the density gradient is perpendicular to the gravitational field or when the density increases from the bottom upward. (pages 127-128)*

Even though such buoyancy-driven flows can arise in electrochemical experiments, e.g. cyclic voltammetry (CV) or chronoamperometry (CA), where a heterogeneous reaction perturbs the local concentration and density profiles, it is usually assumed that mass transport by natural convection is negligible. The latter can be reduced by way of using a suitable orientation of the electrode, or by employing micro- rather than macroelectrodes [3]. As the build-up of density gradients occurs over a comparatively long time scale [2], another way of reducing the influence of natural convection is to perform measurements only at short times.

The transport of each species is governed by a mass-conservation equation,

$$\partial_t C_i = -\nabla \cdot \mathbf{J}_i, \quad (2)$$

where  $t$  is time. In general, charged species are affected by electromigration, and the potential  $\phi$  needs to be eliminated from the system, usually either through the Poisson equation [4] or the electroneutrality approximation [5]. However, electrochemical experiments are typically performed in an excess of supporting electrolyte, which ensures that electrostatic interactions are screened and the migration term in eq. (1) can be neglected [2-4]. As the convective flux is proportional to the fluid velocity  $\mathbf{v}$ , eq. (2) needs to be solved together with the Navier-Stokes and continuity equations, which for small driving forces take the form

$$\nabla \cdot \mathbf{v} = 0; \quad (3)$$

$$\rho_0(\partial_t \mathbf{v} + \mathbf{v} \cdot \nabla \mathbf{v}) = -\nabla p + \eta \nabla^2 \mathbf{v} + (\rho_0 + \Delta \rho) \mathbf{g}, \quad (4)$$

where  $\mathbf{g}$  is the gravitational acceleration,  $p$  is the pressure in the solution,  $\eta$  – the solution viscosity,  $\rho_0$  its unperturbed density, and  $\Delta \rho$  is the density variation due to gradients in concentration and/or temperature. Should the temperature of the solution be inhomogeneous, equations (1)-(4) also need to be coupled with the heat equation,

$$\partial_t T + \mathbf{v} \cdot \nabla T = \chi \nabla^2 T. \quad (5)$$

To a first approximation, the density variation, which drives the flow, is a linear function of the solute concentrations and the temperature:

$$\Delta \rho \approx \rho_0 \left[ \sum_i \beta_i (C_i - C_{i \text{ ref}}) + \frac{1}{\rho_0} \left( \frac{\partial \rho}{\partial T} \right)_p (T - T_{\text{ref}}) \right], \quad (6)$$

where  $\beta_i$  are the densification coefficients of the individual species [6], and  $C_{i \text{ ref}}$  and  $T_{\text{ref}}$  are reference values, namely those before a perturbation was introduced. Eqs. (1)-(6) neglect the variation of all solution properties except the density, and only admit perturbation of the latter in the force term due to gravity – this is known as the Boussinesq approximation [7] and is applicable to small driving forces for the natural convection. Despite the linearization in the solution density, solving the system (1)-(6) together with appropriate boundary conditions is challenging and usually has to be done numerically; furthermore, depending on the system of interest, additional equations may be required. On the other hand, in the limiting cases when convection is driven by variations in temperature or concentration only, eq. (2) or (5) respectively is trivially fulfilled. In this review, we will only describe the various approaches to modelling free convective phenomena in broad strokes and we will focus on recent interesting developments in the field.

### Solute-driven natural convection

The case of solute-driven natural convection has been studied extensively in the literature, including during recent years. Ehrl et al. [8] proposed a computational approach for the case of mass transport by diffusion, solutal convection and migration based on the finite element (FE) method and compared it against experimental data, as well as other models from the literature. The model in Ref. [8] was an extension of an earlier one that considered only forced convection and was proposed by the same group [9]. Our group has also conducted research on this subject – we studied the effect of natural convection on fully supported chronoamperometry at horizontal disc-shaped electrodes of radius  $\sim 1$  mm using eqs. (1)-(4) and a form of eq. (6) that only accounted for the electroactive species [10]. The chronoamperometric oxidation of  $[\text{Fe}(\text{CN})_6]^{4-}$  at a bulk concentration of 9.5 mM was treated and it was shown that in a configuration that, at a time scale of 1 min, natural convection could account for a significant contribution to the total current (17-38%), if the electrode was positioned so that a less dense species was generated at the bottom of the electrochemical cell [10]. This study was concerned mainly with the order of magnitude of the effect and did not consider the difference in diffusivity between the reduced and oxidized form or the influence of the supporting electrolyte on the density profile<sup>1</sup>. The latter has been treated in some detail in a recent paper by Feldberg and Lewis [11], who analysed the density differences arising due to electrochemical reactions under the assumption that the diffusivities of all present species were equal.

This type of natural convection has also been characterized experimentally through methods for imaging the solution velocity [12<sup>\*\*</sup>-13]. Sahore et al. [12<sup>\*\*</sup>] conducted experiments in solutions containing  $[\text{Fe}(\text{CN})_6]^{4-}$  and  $[\text{Fe}(\text{CN})_6]^{3-}$  over concentric ring-disc electrode systems<sup>6</sup> of varying sizes. They observed circulatory flow patterns with maximum velocities of  $\sim 10^{-5} \text{ m}\cdot\text{s}^{-1}$ , the direction of the former in a fixed horizontal plane above the electrodes being dependent on which electrode served as an anode and which – as a cathode, as illustrated in Figure 1. Urban et al. [13] studied the enzymatic oxidation of  $\text{O}_2$  at a vertical electrode in the absence of forced convection and obtained a peak current magnitude that exceeded the diffusion limit. Using particle image velocimetry (PIV), they determined that the local natural convective velocity in the solution had a maximum value of  $\sim 10^{-4} \text{ m}\cdot\text{s}^{-1}$ . They conducted simulations with an added volume force corresponding to a velocity distribution similar to the measured one and obtained better correspondence with the experimental voltammograms.

<sup>1</sup> We need to note that in [10], we used incorrect values for the densification coefficients  $\beta_i$ ; they are taken from [6] and include the contribution of the supporting electrolyte to the solution density, but they pertain to the case with NaOH as the supporting electrolyte, rather than  $\text{KNO}_3$  as in our system. For that reason, the value of the total densification coefficient we use in [10],  $\beta = \beta_{[\text{Fe}(\text{CN})_6]^{3-}} - \beta_{[\text{Fe}(\text{CN})_6]^{4-}} = -5.9 \times 10^{-5} \text{ m}^3 \cdot \text{mol}^{-1}$  differs significantly from the one calculated as  $\beta \approx v_{[\text{Fe}(\text{CN})_6]^{4-}} - v_{[\text{Fe}(\text{CN})_6]^{3-}} = -4.1 \times 10^{-5} \text{ m}^3 \cdot \text{mol}^{-1}$  in our later paper, Ref. [21]. However, as our studies are chiefly concerned with the order of magnitude of convective effects, the precise value of  $\beta$  is only of secondary importance.

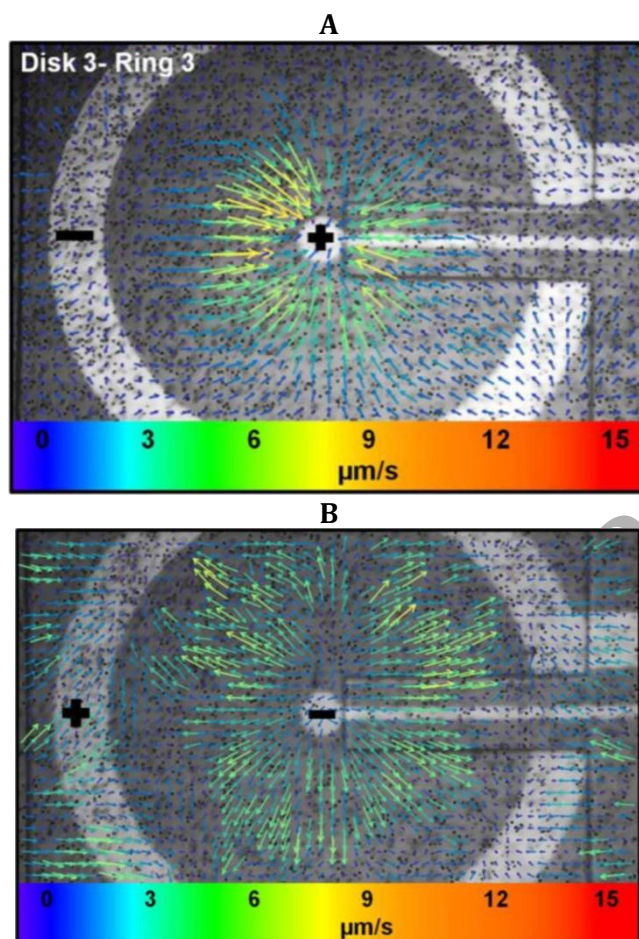


Figure 1. 'Snapshots' of the velocity distribution as visualized via PIV by Sahore et al. [12\*\*] in a ring-disc electrode setup. The solution under study contains 0.095 M  $\text{K}_3\text{Fe}(\text{CN})_6$  and 0.095 M  $\text{K}_4\text{Fe}(\text{CN})_6$  in 0.095 M KCl as the supporting electrolyte.  $\text{K}_3\text{Fe}(\text{CN})_6$  is oxidized at the anode, generating an upward buoyancy force, and  $\text{K}_3\text{Fe}(\text{CN})_6$  is reduced at the cathode. At a fixed vertical distance from the electrodes, the flow direction changes depending on whether the disc serves as the anode (A) or the cathode (B), indicating that the fluid motion is induced by the electrochemical reaction. The radius of the disc is 78  $\mu\text{m}$ ; the inner and outer radii of the ring are 800 and 1000  $\mu\text{m}$ , respectively; the velocity is probed at a height of 320  $\mu\text{m}$  above the plane of the electrodes; the label 'Disk 3 – Ring 3' reflects that the same experiment was conducted with ring-disc electrodes of various sizes. Reprinted with permission from Ref. [12\*\*]. Copyright 2016, The Electrochemical Society.

### Temperature-driven natural convection

As eq. (6) implies, local variations in temperature can also drive natural convective flows; this is known as Rayleigh-Bénard convection. Amaya-Ventura and Rodríguez-Romo [14] demonstrated the applicability of the lattice Boltzmann method to an enzymatic reaction occurring at the membrane interface between an immobilized enzyme and a solution. The response of the system was monitored through electrodes at the bottom of the porous enclosure containing the enzyme. Due to the large imposed temperature difference between the electrodes and the environment ( $\Delta T \sim 30$  K), the authors neglected the influence of the reaction on  $\rho$  in eq. (6), thus decoupling the governing equations for the species concentrations from those for momentum and temperature.

Thermal convection in electrochemical systems has been studied in our group [15-16], specifically problems with imperfect thermostating, which was modelled as an initial temperature difference ( $|\Delta T| \sim 5$  K) between the solution and its environment. Detailed simulations of the heat and momentum transfer between an idealized measurement cell for

scanning electrochemical microscopy (SECM) and the surrounding air showed that, in the absence of thermostating, thermal equilibration has a characteristic time scale of  $\sim 1000$  s and may generate flows with a maximum velocity of  $\sim 10^{-4}$  m·s $^{-1}$  [15]. A later work [16] dealt with a simpler model of a cell insulated from the environment and thermostatted from below through a solid substrate with spatially inhomogeneous thermal conductivity. The simulations in Ref. [16] indicate that the profile of the latter influences the pattern and intensity of the observed convective flows, which reach a maximum local velocity of  $\sim 10^{-3}$  m·s $^{-1}$ . ‘Snapshots’ of the complicated evolution of the temperature and velocity profile next to a disc-shaped substrate of high thermal conductivity with an insulating band are shown in Figure 2.

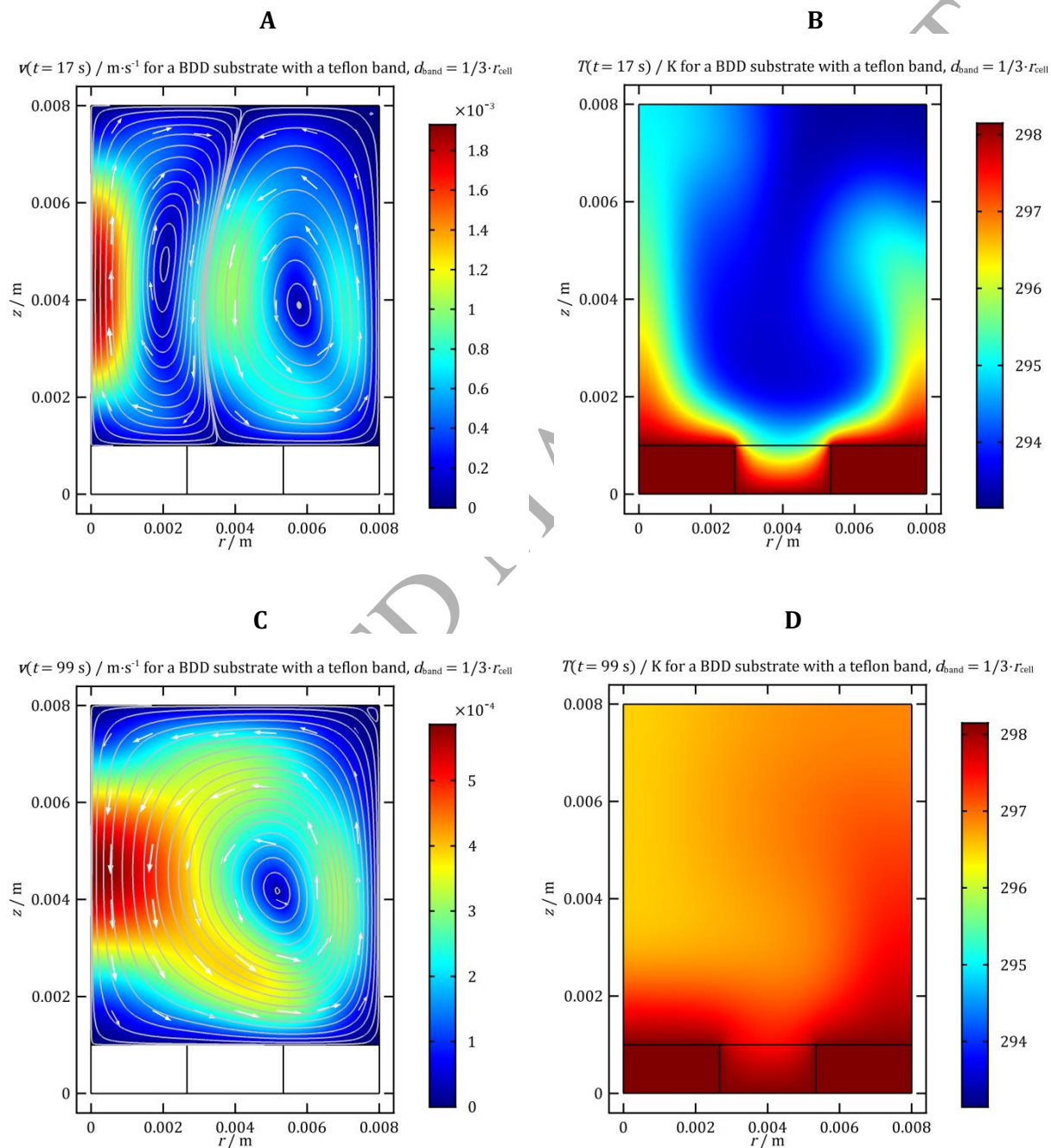


Figure 2. Profiles of  $v$  and  $T$  for a disc-shaped boron-doped diamond substrate of radius  $r_{\text{cell}}$  with a teflon band of width  $d_{\text{band}}$  ( $d_{\text{band}}/r_{\text{cell}} = 1/3$ ); the flow arises because the solution is initially colder than the substrate by  $\Delta T = 5$  K. The temperatures of both the solution and the substrate are initially homogeneous, the latter being  $T_{\text{thermostat}}$ ; the substrate's bottom surface is maintained at  $T_{\text{thermostat}}$  throughout the simulation. The velocity and temperature distributions go through a complicated evolution, which is partly illustrated in the ‘snapshots’ A–D, taken at the two



maxima of the volume-averaged solution velocity absolute value,  $t = 17$  s and  $t = 99$  s. **A** illustrates the velocity distribution with streamlines illustrating the two transient convective rolls; **B** – the temperature distribution that this flow pattern brings about. **C** shows the single-roll velocity pattern that eventually emerges as a result from the merging of the two rolls in **A**; **D** demonstrates the profile of  $T$  corresponding to it. The length of the arrows in **A** and **C** is proportional to the natural logarithm of the absolute value of the velocity at the given point. For this simulation, Reproduced from Ref. [16] by permission of the PCCP owner societies.

In another work on thermal convection, Huang and Chao [17\*] simulated the flow patterns generated by local heating from two wires situated at the bottom of a liquid layer. They analysed the behaviour of the system as a function of the relevant dimensionless numbers for the problem and constructed a stability map of the possible flow regimes. From their simulations, they determined the resolution, defined through the minimum separation between the wires at which the flows generated by them are distinguishable, and obtained good agreement with experimental data. Furthermore, they showed that, if the dimensionless numbers characterizing the flow were in a particular region, the flow resolution could be tuned by varying the experimental conditions.

### Temperature and solute-driven natural convection

Although few in number, there exist recent computational studies which deal with both thermal and solute-driven convection. Pismensky et al. [18] studied the effect of combined natural and forced convection on the mass transport in electromembrane cells for desalination working under chronoamperometric and chronopotentiometric conditions. Following Taylor and Sharman [19], they expressed the electric current in their simulations of chronopotentiometry through a stream function, by analogy with incompressible fluid flow. They derived an expression relating the current and the concentration for a binary electrolyte under the electroneutrality approximation; their approach was clarified in a later paper [20]. In their model, the desalination and Joule heating at the membrane electrodes reduces the local solution density and generates a buoyancy force. Pismensky et al. [18] varied the intensity of the forced flow in the cell and estimated the conditions for the onset of natural convective flows; their simulated chronopotentiograms showed satisfactory agreement with experimental data. Our group [21] studied the cyclic voltammetry and chronoamperometric oxidation of  $[\text{Fe}(\text{CN})_6]^{4-}$  at vertical electrodes of various sizes, taking into account both solute-driven convection and thermal convection due to the intrinsic heat of the chemical reaction<sup>2</sup>. The latter effect was found to be negligible under all studied conditions because the temperature change induced by the electrochemical reaction leads to a much smaller density perturbation than the local variation in the concentration of the electroactive species. Figure 3 shows the concentration, temperature and velocity distributions at two moments in time during a simulated chronoamperometric oxidation of  $[\text{Fe}(\text{CN})_6]^{4-}$  at a disc-shaped electrode.

<sup>2</sup> We need to clarify our choice of densification coefficients  $\beta_i$  in Ref. [21]. Due to a technical mistake on our part, the left-hand side of eq. (35) reads  $\rho - \rho_0$  rather than the correct  $(\rho - \rho_0)/\rho_0$ . Furthermore, the expression that we use for the overall densification coefficient in Ref. [21],  $\beta = v_{\text{Ox}} - v_{\text{Red}}$ , implicitly neglects the difference between the density of the pure solvent,  $\rho_s$ , and that of the unperturbed solution,  $\rho_0$  – taking that difference into account would yield  $\beta = (v_{\text{Ox}} - v_{\text{Red}})\rho_s/\rho_0$ , i.e. a value differing from ours by a factor of  $\rho_s/\rho_0 \sim 0.97$ . However, the reported values for the molar volumes  $v_{\text{Ox}}$  and  $v_{\text{Red}}$  have significantly larger dispersion, translating into an error of  $\sim 30\%$  in the difference  $v_{\text{Ox}} - v_{\text{Red}}$ , see Ref. [22], making the factor  $\rho_s/\rho_0$  immaterial.



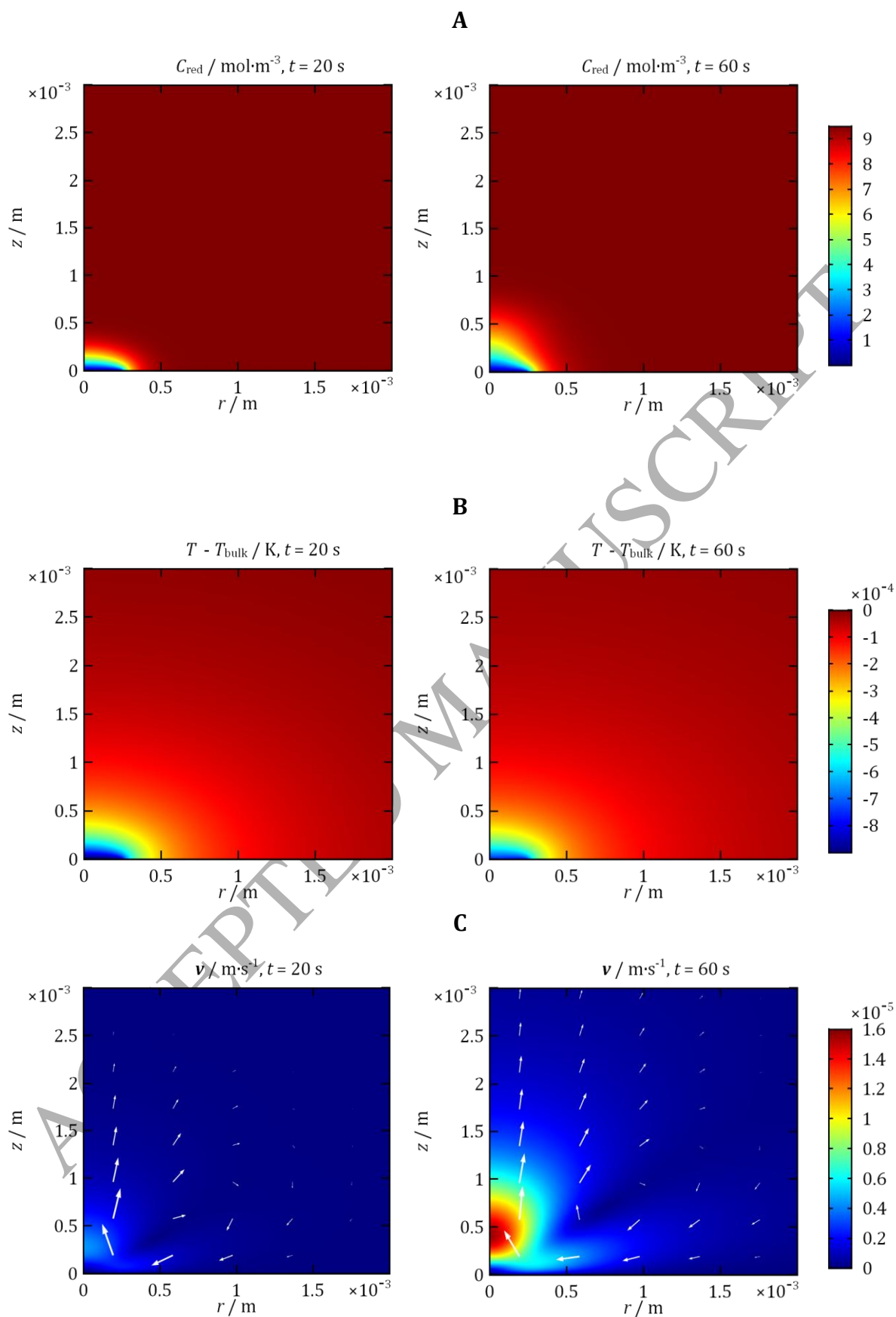


Figure 3. Profiles of the concentration (A), the difference between the solution temperature and its initial value,  $T_{\text{bulk}}$  (B) and the velocity (C) at  $t = 20$  and  $60 \text{ s}$  for a chronoamperometric oxidation of  $[\text{Fe}(\text{CN})_6]^{4-}$  at a disc-shaped electrode of radius  $0.25 \text{ mm}$ . The simulated cylindrical cell extends significantly beyond the characteristic

thermal length; it is assumed to be perfectly thermally insulated; apart from the electrode surface, it is also electrically insulated. The length of the arrows representing the velocity vector is proportional to the natural logarithm of  $|\mathbf{v}|$ . Note that the distortion of the concentration profile at long times that occurs in the vicinity of the axis of symmetry, where the flow is most intense. The disturbance in concentration due to the chemical reaction spreads much more slowly than that in temperature, but the magnitude of the latter is such that it has a negligible influence over the convective flow and the overall mass flux through the electrode [21]. Reprinted with permission from Ref. [21]. Copyright 2016, American Chemical Society.

### **Experimental approaches for minimizing convection**

A way of minimizing the contribution of natural convection to electrochemical measurements is to conduct them in highly viscous media [1]. Taking advantage of this, Aoki and co-workers [23-24] performed voltammetric studies in solutions with added sodium alginate and demonstrated that convective currents were suppressed. They measured the voltammetric peak current, the solution electrical conductivity and viscosity as a function of the polymer concentration and found that the former two were approximately constant, while the latter increased greatly. Aoki et al. [24] attributed these observations to the fact that the pores in the polymer network were much larger than the diffusing species and thus hardly affected their diffusion. Kang and Hwang [25] conducted cyclic voltammetry in agarose gels and also concluded that the polymer reduced free convection without affecting the diffusion coefficient of the species under study. Park et al. [26] performed CV under conditions of reduced vibrations, thus obtaining better reproducibility of the measured current at low scan rates; they ascribed this improvement to reduced natural convection.

### **Electrochemical sensors utilizing natural convection**

Electrochemical sensors utilizing natural convection have been developed in recent years. Sun and Agafonov [27] analyzed the effects of solutal natural convection, diffusion and migration in a 4-electrode electrochemical accelerometer via FE simulations and compared the results obtained with the Boussinesq approximation to those for compressible flow. They came to the conclusion that the former was adequate for calculating the current at a single electrode, but not the difference between the currents at the two cathodes, which is used in measuring external accelerations. Contento and Semancik [28\*] constructed a sensor consisting in a disc-shaped electrode of radius  $\sim 25 \mu\text{m}$  and an underlying microheater. These authors performed CV at elevated temperatures (up to 354 K) and observed a marked improvement of the signal, which they showed to be partly due to thermal convection. Boika and Zhao [29] constructed a heated SECM tip and saw that tip-substrate approach curves varied substantially with substrate conductivity at small separations.

### **Natural convection in fuel and thermogalvanic cells**

Natural convective effects have been considered in electrochemical fuel cells. Antunes and Skrzypkiewicz [30\*] observed that gas transport in a direct carbon solid fuel cell is enhanced by natural convection due to a pressure gradient brought about by the Boudouard reaction. Sikovsky et al. [31] simulated the heat transfer in an aluminium-air fuel cell, taking into account Joule heating and the heat flux due to the electrochemical reaction. They observed that thermal convection leads to fluctuations in the cell voltage, which were qualitatively confirmed by experimental data.

Thermogalvanic cells convert heat into electrical power and can be used to harvest waste heat [32-33], the downside being their typical efficiency of well below 1% [32]. In devices of this type, a temperature difference between two electrodes generates a potential difference which in turn generates an electrical current. Recent simulations of such cells and demonstrated that natural convection can improve their efficiency several times [32-33]. Salazar et al. [32] modelled the stationary mass, heat and momentum transport in a thermogalvanic cells, taking into account only thermal convection due to the large temperature difference between the two electrodes (60 K). Their simulations, which showed a five-fold increase in cell efficiency upon inclusion of natural convection in the model, compared favourably to literature experimental data. Gunawan et al. [33] observed saw that the maximum power output of a thermogalvanic cell depended strongly on its configuration, again attributing this to natural convection.

### **Bubble-induced convection**

A problem of importance to many industrial processes is the bubble-induced convection in electrochemical systems [34\*]. Electrogenerated bubbles can affect the efficiency of such processes by inducing mixing, but also by altering the local electrical conductivity of the medium [34\*]. However, we should note that the description of such two-phase flows requires more involved equations than (1)-(6), see for instance Ref. [35].

Experimental and computational results pertaining to the common case of bubble convection at vertical electrodes have been covered in a recent review by Hreiz et al. [34\*] that highlights the many difficulties of investigating such systems. Schillings et al. [36\*] recently simulated the bubble-induced flow in water electrolysis under conditions of forced and natural convection and obtained adequate agreement with experimental results.

Interestingly, a number of recent studies have eliminated the contribution of bubble-induced convection by performing experiments in reduced gravity [37-39]. Mandin and co-authors have applied this technique to the electrolysis of water [37] and  $\text{CuSO}_4$  [38], and Sakuma et al. [39] minimized convection in is manner in order to focus on the effect of electrode wettability.

### **Studies with an additional external force**

Several recent articles have investigated convection driven by both the buoyancy force that eq. (4) considers and an external force,  $F_{\text{ext}}$ . Strictly speaking, this case falls under the label of mixed convection, as it contains contributions from both natural and forced flows.

Wang and co-workers [40] observed improved rate of electrodeposition of copper and nickel under centrifugal acceleration aligned with the electric field. They also recently published a review on the subject of electrochemistry in centrifugal fields [41].

Natural convection is of particular importance for the important industrial processes of electrowinning and electrorefining, e.g. of copper. Free convective flows, typically combined with forced ones, not only affect the transport of metal ions, but also play a role in the transport of anode slime particles, which are a major source of contamination of the purified metal in electrorefining [42\*-43\*]. Zeng et al. have recently performed detailed simulations of both of these processes on a laboratory scale, for cells of a conventional [42\*] and non-standard [43\*-44] designs. Najminoori et al. [45] have studied the free convective flow driven by concentration gradients and gas bubbles in a copper electrowinning cell via simulations and experiments.

An interesting area of research is the study of electrochemical systems subjected to magnetic fields. Electrochemical studies most often consider only the Lorentz force,  $F_{\text{Lorentz}} = \mathbf{J} \times \mathbf{B}$ , where  $\mathbf{J}$  is the electrical current density and  $\mathbf{B}$  is the magnetic induction. Work concerning Lorentz force effects has been summarized by Monzon and Coey [46]; in another paper [47], they reviewed the effect of magnetic field gradients in electrochemistry. More recently, the effect of combined natural and magnetohydrodynamic convection on the electrodeposition of various materials has been studied, e.g. for Zn-Ni alloys [48] and copper [49-50]. In particular, references [49-50] contain treatment of various magnetoelectrolysis problems by way of simulations and experiments, examining different orientations of the Lorentz force with respect to the buoyancy force. Baczynski and co-authors dealt with Lorentz-force effects in bubble-driven convection at gas-evolving electrodes [51-52]. In an experimental study, they showed that applying a magnetic field to a cell for water electrolysis can improve its efficiency by enhancing bubble detachment [51]. In another paper [52], they examined the effect of buoyancy and Lorentz forces on the evolution of a single  $\text{H}_2$  bubble via both simulations and experiments.

### **Studies that utilize the analogy between heat and mass transfer**

As under conditions of full support and appropriate boundary conditions mass and heat transfer are governed by equations of the same form, it is possible to gain insight into one process by probing the other. It is particularly useful that, if non-dimensionalized appropriately, the heat and mass flux obey analogous functional dependences [7]; for a discussion of the limitations of this analogy, see Section 22.3 in Ref. [7]. Electrochemical experiments enable the study in reduced scale of systems that are otherwise difficult to probe – for example, Lim and Chung [53] have used an electrochemical cell with a rod electrode to model the heat transfer in a chimney. Moon and Chung [54] have studied the solutal time-dependent Rayleigh-Bénard flow in a copper electroplating experiment as a model for the cooling of the molten core of a nuclear reactor during an accident. In another paper, the same group [55] modelled the natural convective heat transfer past two staggered cylinders through an electrochemical experiment. In another recent study, Vogt [56] used the same analogy to derive expressions for the dimensionless mass flux at various conditions from correlations formulated for the heat flux.

### **Spontaneous convection?**

In a paper from 2001, Amatore et al. [57] introduced the term ‘spontaneous convection’, which they define as a mode of mass transport due to ‘microscopic chaotic motion’ in macroscopically still solutions, underlining that it is distinct from forced or natural convection. The concept has been invoked in various recent papers, e.g. Refs. [25, 58-65]. The authors’ [57] model for spontaneous convection ‘. . . is based on a seminal idea introduced by Levich, and shows that in macroscopically still solutions microscopic chaotic motion has the same effect as an apparent [distance-dependent] diffusion coefficient . . .’. The model references Levich’s monograph [1] and utilizes equations appearing in Chapter III of that book. However, Levich’s equations cited in Ref. [57] relate to the case of a macroscopic *turbulent* flow past a solid wall; we were unable to find any discussion of this type of microscopic chaotic motion in *stagnant*

solutions in Ref. [1]<sup>3</sup>. Below, we compare Levich's model and that of [57], highlighting apparent contradictions in the latter.

Levich's model, which Amatore and co-authors adopt, posits a four-layer structure of the concentration profile under conditions of turbulent flow next to an infinite solid flat plane, as illustrated schematically in Figure 4A. Large normal distances from the wall ( $y > d$ ) correspond to the region of *developed turbulence*, where the solution is well-mixed and the concentration is homogeneous. Closer to the wall ( $d > y > \delta_0$ ), there is a *turbulent boundary layer* in which both mass and momentum transport occur mainly via turbulent eddies with a characteristic length scale of  $y$ . The mass flux  $j$  can be written as  $j \propto D_{\text{turb}} \partial C / \partial y$ , where  $D_{\text{turb}}$  is an effective diffusion coefficient that takes into account turbulent mass transport; for this region,  $D_{\text{turb}} \propto y$ . At still smaller  $y$  ( $\delta_0 > y > \delta$ ), in the *viscous sub-layer*, momentum transport occurs predominantly via molecular viscosity, but mass transport is still mostly through turbulent eddies, whose characteristic scale is  $y^2$ ; within this sub-layer,  $D_{\text{turb}} \propto y^4$ . In this view of turbulence, the retarding effect of the solid wall is strong enough to make molecular diffusion the dominant mode of mass transport only in the *diffusion sub-layer* of thickness  $\delta$ ,  $\delta < \delta_0$ . For a detailed discussion of the subject, see Sections 4 and 24-25 of Levich's book [1].

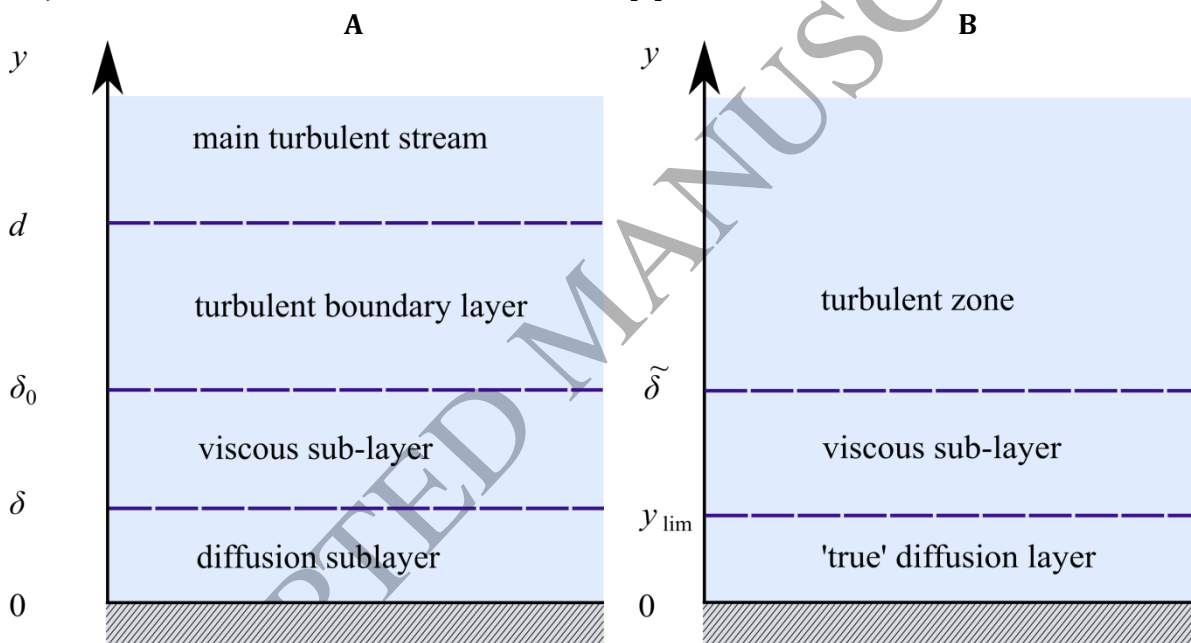


Figure 4. Layered structure of the concentration profile next to a flat wall. **A** – for turbulent flow, as given in Levich's monograph [1]. **B** – our visual representation of the structure of the concentration profile for the model of Amatore et al. [57]; the thickness  $\tilde{\delta}$  is not given a symbol in [57].

Citing Levich [1], Ref. [57] explains discrepancies between data from electrochemical experiments and a simple diffusion-only mass transport model by postulating that macroscopically still solutions exhibit 'microscopic turbulence'. The latter is assumed to give rise to viscous and 'true' diffusion sub-layers next to the surface of a flat macroelectrode, with boundaries at normal distances of  $y = \tilde{\delta}$  and  $y = y_{\text{lim}}$ , respectively (Figure 4B). Amatore et al. suppose that for the cases of interest the concentration reaches its bulk value within a distance  $\tilde{\delta}$  (our notation) from the surface and exclusively consider  $y < \tilde{\delta}$ . For the viscous sub-layer, they assert that there is a convective contribution to the diffusion coefficient,  $D_{\text{app}} = D + D_{\text{conv}}$ , and that  $D_{\text{conv}} \propto (y/y_{\text{lim}})^4$ . However, as pointed out above, this functional dependence on distance is for

<sup>3</sup> We consulted both the English translation of the book [1] and the second edition in Russian on which it is based [66].

the case of turbulent flows at *large Reynolds* numbers (typically, at  $Re \gtrsim 1500$  [1]), namely, ones that involve intense macroscopic fluid motion. Applying the equation in question to a macroscopically still solution, for which the Reynolds number is zero, represents a major leap from the model in Ref. [1]. We next discuss the problematic points which arise as a consequence of that jump.

As we see from the comparison between the models in [1] and [57], the role of  $y_{\text{lim}}$  is equivalent to that of  $\delta$ , i.e., both give the thickness of the layer in which diffusion is the predominant mode of mass transport. Thus, we can take the value of  $y_{\text{lim}} = 2.3 \times 10^{-4} / 1.108 = 2.08 \times 10^{-4}$  m from [57] and use Levich's equation 25.16,  $\delta = (10^3 D \nu^3 / \gamma)^{1/4} / \nu_0$ , to determine the velocity of the turbulent eddies characteristic of the flow in Levich's model,  $\nu_0$ ; here,  $\nu$  is the kinematic viscosity of the medium, and  $\gamma$  is a numerical constant 'not greatly different from unity' [1]. Specifically, as comparison between eq. 25.11 in Ref. [1] and eq. 9 in Ref. [57] shows, Amatore et al. implicitly set  $\gamma = 1$ . In this way, we obtain that for the system in question, the *turbulent eddies* in a *macroscopically still solution* postulated in [57] would have to have a characteristic velocity  $\nu_0$  of the order of  $10^{-3}$  m·s<sup>-1</sup>. Moreover, accepting the analogy with Levich's model, we see that in the presumed turbulent zone,  $y > \delta$ , there are eddies of characteristic size  $l \sim y$ .  $\delta$  itself is defined to be the distance from the surface at which the local Reynolds number for the eddies is of the order of 1,  $Re = \nu_0 l(x) / \nu = \nu_0 \delta / \nu \sim 1$ . It follows that  $\delta = a \nu / \nu_0$ , where  $a \sim 10$  [1], and for the case of Amatore et al. [57],  $\delta \sim 10 \times 10^{-6} / 10^{-3} \sim 10^{-2}$  m, which means that the smallest eddies in the turbulent sublayer have a characteristic size of the order of 1 cm and a characteristic velocity of the order of  $10^{-3}$  m/s! Such large-scale motion is incompatible with the core model assumption that the solution is *macroscopically still*, and eddies of this size and velocity could be observed by standard techniques for flow characterization, e.g., PIV, as seen for example in Ref. [67]. Perhaps in Ref. [57], the authors have adopted the Levich model [1] for eddy mass transport without taking into account that the eddies in question are caused by the bulk turbulent flow<sup>4</sup>, and are therefore not present in a stagnant solution?

Notwithstanding the uncertain theoretical (and historical) basis of the equation for  $D_{\text{conv}}$  and its dependence on the fourth power of distance, Amatore and colleagues performed a number of careful, rigorous and insightful experiments that suggest the involvement of convective effects under nominally diffusion-only conditions. In [57], the observed deviation of chronoamperometric currents at a macroelectrode from Cottrellian behaviour was satisfactorily accounted for using the expression for  $D_{\text{conv}}$  referenced above when  $\delta$  was treated as an empirical adjustable parameter and  $D$  was chosen from a fit of the data at short times. In the follow-up papers to [57], CA was performed at macro- [68] and micro-sized disc electrodes [69]; CV was conducted for disc electrodes of various sizes [70]; concentration profiles were imaged in the vicinity of microdiscs [71]. Microband electrodes were considered as well – CV and CA were performed at a single electrode of this type [64], and CA was done in the case of a microband array [60]. The influence of electromigration was also studied in the same context

<sup>4</sup> Consult [1], page 22: "Together with these large scale eddies, turbulent flow also includes eddies of smaller scale  $\lambda$ , with lesser velocities  $\nu_\lambda$ . . . . The superposition of large scale eddies on each other creates small scale eddies, for which the Reynolds numbers rapidly decrease with decreasing  $\lambda$ ". In the Russian edition [66], on page 31, this passage reads "Наряду с этими крупномасштабными пульсациями в турбулентном потоке представлены пульсации меньшего масштаба  $\lambda$ , имеющие меньшие скорости  $\nu_\lambda$ . . . . Наложение друг на друга крупномасштабных пульсаций порождает мелкомасштабное пульсационное движение, для которого число Рейнольдса быстро снижается с уменьшением  $\lambda$ ".

for the case of macroelectrodes [72-73]. Crucially, concentration profiles near electrodes were probed with a separate amperometric ultramicroelectrode [57, 68, 70, 72-73] (of radius between  $\approx 0.5$  [70] and  $5\ \mu\text{m}$  [73]) or with SECM [60, 64, 69-71]; good agreement was found between the experimental currents and concentrations and the predictions of the 'spontaneous convection' model.

In their later papers [60-62, 64-65, 69-71, 73] Amatore and co-authors refer to the same phenomenon, which they assert to be the source of the deviation from purely diffusional behaviour, as 'natural convection' and 'spontaneous natural convection'. Their experiments were seemingly not thermostatted and hence  $\delta$  'depends on the external environment and other phenomena such as local vibrations and temperature gradients' [64] and its value is reported to be between  $135$  [68] and  $250\ \mu\text{m}$  [64]. The experiments are important as they provide evidence for the importance of convection in electrochemical experiments performed in a nominally quiescent solution and have clear implications for 'diffusion-only' voltammetry in general and SECM in particular.

## 2. Conclusions

As the research summarized here indicates, recent years have seen the inclusion of natural convection in studies of a broad spectrum of electrochemical phenomena, ranging from thermogalvanic and fuel cells to sensors. Natural convective effects are routinely taken into account in certain areas, e.g., the modelling of the electrorefining process, but are often ignored in electroanalytical contexts, not always with rigorous justification. In our opinion, a promising direction for future research is to seek quantitative characterization of natural convective contributions in experiments, particularly within the fields of electroanalysis and physical electrochemistry.

**Acknowledgements.** J.K.N. thanks the Clarendon Fund and Trinity College of the University of Oxford for a Clarendon-Titley scholarship.

## References and recommended reading

Papers of particular interest, published within the period of review, have been highlighted as:

\* Paper of special interest

\*\* Paper of outstanding interest

1. V.G. Levich, *Physicochemical Hydrodynamics*, Prentice-Hall, Inc., Englewood Cliffs, NJ, 1962.
2. A.J. Bard, L.R. Faulkner, *Electrochemical Methods: Fundamentals and Applications*, Second edition, Wiley, New York, 2001.
3. X. Gao, J. Lee, H.S. White, Natural Convection at Microelectrodes, *Anal. Chem.* 67 (1995) 1541-1545.
4. R.G. Compton, E. Laborda, K.R. Ward, *Understanding Voltammetry: Simulation of Electrode Processes*, Imperial College Press, London, 2014.



5. E.J.F. Dickinson, J.G. Limon-Petersen, R.G. Compton, The electroneutrality approximation in electrochemistry, *J. Solid State Electrochem.* 15 (2011) 1335-1345.
6. J.R. Selman, J. Newman, Free-Convection Mass Transfer with a Supporting Electrolyte, *J. Electrochem. Soc.* 118 (1971) 1070-1078.
7. R.B. Bird, W.E. Stewart, E.N. Lightfoot, *Transport Phenomena*, Second Edition, Wiley, New York, 2002.
8. A. Ehrl, G. Bauer, V. Gravemeier, W.A. Wall, A computational approach for the simulation of natural convection in electrochemical cells, *J. Comput. Phys.* 235 (2013) 764-785.
9. G. Bauer, V. Gravemeier, W.A. Wall, A stabilized finite element method for the numerical simulation of multi-ion transport in electrochemical systems, *Comput. Methods Appl. Mech. Engrg.* 223-224 (2012) 199-210.
10. K. Ngamchuea, S. Eloul, K. Tschulik, R.G. Compton, Advancing from Rules of Thumb: Quantifying the Effects of Small Density Changes in Mass Transport to Electrodes. Understanding Natural Convection, *Anal. Chem.* 87 (2015) 7226-7234.
11. S. W. Feldberg, E. R. Lewis, Concentration and Density Changes at an Electrode Surface and the Principle of Unchanging Total Concentration, *J. Electrochem. Soc.* 163 (2016) H3167-H3172.
12. \*\* V. Sahore, A. Kreidermacher, F.Z. Khan, I. Fritsch, Visualization and Measurement of Natural Convection from Electrochemically-Generated Density Gradients at Concentric Microdisk and Ring Electrodes in a Microfluidic System. *J. Electrochem. Soc.* 163 (2016) H3135-H3144.  
Chronoamperometric and chronopotentiometric experiments are performed with mixtures of  $K_3[Fe(CN)_6]$  and  $K_4[Fe(CN)_6]$  at ring-disc electrode systems. Convective velocities of up to  $10^{-5}$  m/s are probed in a horizontal plane using PIV; the direction of flow within that plane is observed to change upon reversal of the polarity of the electrodes.
13. J. Urban, A. Zloczewska, W. Stryczniewicz, M. Jönsson-Niedziolka, Enzymatic oxygen reduction under quiescent conditions — the importance of convection, *Electrochem. Commun.* 34 (2013) 94-97.
14. G. A. Amaya-Ventura, S. Rodríguez-Romo, LBM for cyclic voltammetry of electrochemically mediated enzyme reactions and Rayleigh-Bénard convection in electrochemical reactors, *Heat Mass Transf.* 48 (2012) 373-390.
15. J.K. Novev and R.G. Compton, Convective heat transfer in a measurement cell for scanning electrochemical microscopy, *Phys. Chem. Chem. Phys.* 18 (2016) 29836-29846.
16. J.K. Novev and R.G. Compton, Thermal Convection in Electrochemical Cells. Boundaries with Heterogeneous Thermal Conductivity and Implications for Scanning Electrochemical Microscopy, *Phys. Chem. Chem. Phys.* 19 (2017) 12759-12775.
17. L.-T. Huang, L. Chao, The flow patterning capability of localized natural convection, *Phys. Chem. Chem. Phys.* 18 (2016) 25380-25387.  
Rayleigh-Bénard flows are studied experimentally and via FE simulations. A state diagram of the possible flow patterns is obtained in terms of the Grashof ( $Gr$ ) and Prandtl ( $Pr$ ) numbers, which quantify respectively the ratios of viscous to buoyancy forces and of kinematic viscosity to thermal diffusivity. It is shown that in a particular region of  $Pr$  and  $Gr$ , the properties of the flow patterns can be reliably controlled by variation of the dimensionless numbers.
18. A.V. Pismensky, M.K. Urtenov, V.V. Nikonenko, P. Sistat, N.D. Pismenskaya, A.V. Kovalenko, Model and Experimental Studies of Gravitational Convection in an Electromembrane Cell, *Russ. J. Electrochem.* 48 (2012) 756-766.
19. G.I. Taylor, C.F. Sharman, A Mechanical Method for Solving Problems of Flow in Compressible Fluids, *Proc. Roy. Soc. A* 121 (1928) 194-217.
20. S.A. Mareev, V.S. Nichka, D. Yu. Butylskii, M. Kh. Urtenov, N.D. Pismenskaya, P.Yu. Apel, V.V. Nikonenko, Chronopotentiometric Response of an Electrically Heterogeneous Permselective Surface: 3D Modeling of Transition Time and Experiment, *J. Phys. Chem. C* 120 (2016) 13113-13119.

21. J.K. Novev, S. Eloul and R.G. Compton, Influence of Reaction-Induced Thermal Convection on the Electrical Currents Measured in Chronoamperometry and Cyclic Voltammetry, *J. Phys. Chem. C* 120 (2016) 13549-13562.
22. Y. Marcus, *Ion Properties*, Marcel Dekker, New York, 1997.
23. B. Wang, K.J. Aoki, J. Chen, T. Nishiumi, Slow scan voltammetry for diffusion-controlled currents in sodium alginate solutions, *J. Electroanal. Chem.* 700 (2013) 60-64.
24. K. Aoki, B. Wang, J. Chen, T. Nishiumi, Diffusion coefficients in viscous sodium alginate solutions, *Electrochim. Acta* 83 (2012) 348-353.
25. H. Kang, S. Hwang, Electrochemical Characterization of the Hydrophobic Interaction and the Natural Convection within Agarose Gel, *Int. J. Electrochem. Sci.* 10 (2015) 9706-9713.
26. K. Park, E. Kim, J.H. Park, S. Hwang, Influence of an active vibration isolator and electrochemical cell design on electrochemical measurements to minimize natural convection, *Electrochem. Commun.* 82 (2017) 93-97.
27. Z. Sun, V. M. Agafonov, Numerical Modeling of a Four-Electrode Electrochemical Accelerometer Based on Natural Convection: The Boussinesq Flow Model Vs. The Compressible Flow Model, *Russ. J. Electrochem.* 48 (2012) 835-842.
28. \* N.M. Contento, S. Semancik, Thermal characteristics of temperature-controlled electrochemical microdevices, *Sens. Actuators B* 225 (2016) 279-287.  
A sensor consisting of a microdisc electrode and an underlying microheater is constructed. CV of a model analyte is performed at elevated temperatures, and an enhancement of the electrochemical signal is observed – as the temperature is raised from  $\approx 293$  to  $\approx 353$  K, the peak voltammetric current sees a threefold increase. The voltammetric currents obtained under these conditions are compared against FE simulations – a diffusion-only model and one that includes thermal convection, the latter giving currents closer to the experimental.
29. A. Boika, Z. Zhao, First principles of hot-tip scanning electrochemical microscopy: Differentiating substrates according to their thermal conductivities, *Electrochem. Commun.* 68 (2016) 36-39.
30. \* R. Antunes, M. Skrzypkiewicz, Chronoamperometric investigations of electrooxidation of lignite in direct carbon bed solid oxide fuel cell, *Int. J. Hydrogen Energy* 40 (2015) 4357-4369.  
 $I(t)$  curves for the chronoamperometric oxidation of CO at the anode of a direct carbon bed solid oxide fuel cell are fit to a model expression derived under the assumption that CO is transported by diffusion and undergoes irreversible oxidation; the best-fit effective diffusion coefficient is of the order of  $10^{-2}$  m<sup>2</sup>/s. It is proposed that this high value is due to the reverse Boudouard reaction occurring at the anode,  $C + CO_2 \rightarrow 2CO$ , which induces a pressure gradient and therefore a natural convective flow in it. Mass transfer is described with a simple 1D-model based on the assumption that convection is the predominant mode of transport. The convective velocity is described through Darcy's law, as the study is concerned with flow through a porous medium.
31. D.P. Sikovsky, S. M. Kharlamov, V.I. Palymsky, K.G. Dobroselsky, M.G. Vlasenko, and B.B. Ilyushin, Heat Transfer and Thermohydrodynamic Fluctuations in Aluminum–Air Fuel Cell, *J. Eng. Thermophys.* 24 (2015) 386-397.
32. P.F. Salazar, S. Kumar, B.A. Cola, Design and optimization of thermo-electrochemical cells, *J. Appl. Electrochem.* 44 (2014) 325-336.
33. A. Gunawan, H. Li, C.-H. Lin, D.A. Buttry, V. Mujica, R.A. Taylor, R.S. Prasher, P.E. Phelan, The amplifying effect of natural convection on power generation of thermogalvanic cells, *Int. J. Heat Mass Transfer* 78 (2014) 423-434.
34. \* R. Hreiz, L. Abdelouahed, D. Fünfschilling, F. Lapique, Electrogenated bubbles induced convection in narrow vertical cells: A review, *Chem. Eng. Res. Des.* 100 (2015) 268-281.

Convection induced by electrogenerated bubbles is reviewed for the case of vertical electrodes. The advantages and limitations of the various computational fluid dynamics methods and experimental techniques are discussed in detail.

35. A. Sokolichin, G. Eigenberger, A. Lapin, Simulation of buoyancy driven bubbly flow: Established simplifications and open questions, *AIChE J.* 50 (2004) 24-45.

36. \* J. Schillings, O. Doche, J. Deseure, Modeling of electrochemically generated bubbly flow under buoyancy-driven and forced convection, *Int. J. Heat Mass Transf.* 85 (2015) 292-299.

Simulations of the bubbly flow in water electrolysis at vertical electrodes are performed with a 2D two-phase mixture (drift-flux) model solved via FE; the cases of both free and forced convective flow in the cell are considered. The obtained velocity profiles are shown to agree well with experimental data from the literature. A scaling law for the thickness of the bubble plumes is derived.

37. P. Mandin, Z. Derhoumi, H. Roustan, W. Rolf, Bubble Over-Potential During Two-Phase Alkaline Water Electrolysis, *Electrochim. Acta* 128 (2014) 248-258.

38. Z. Derhoumi, P. Mandin, H. Roustan, R. Wüthrich, Experimental investigation of two-phase electrolysis processes: comparison with or without gravity, *J. Applied Electrochem.* 43(2013) 1145-1161.

39. G. Sakuma, Y. Fukunaka, H. Matsushima, Nucleation and growth of electrolytic gas bubbles under microgravity, *Int. J. Hydrogen Energy* 39 (2014) 7638-7645.

40. M. Wang, Z. Wang, Z. Guo, Deposit structure and kinetic behavior of metal electrodeposition under enhanced gravity-induced convection, *J. Electroanal. Chem.* 744 (2015) 25-31.

41. M. Wang, Z. Wang, X. Gong, Z. Guo, Progress toward Electrochemistry Intensified by using Supergravity Fields, *ChemElectroChem* 2 (2015) 1879-1887.

42. \* W. Zeng, S. Wang, M.L. Free, Experimental and Simulation Studies of Electrolyte Flow and Slime Particle Transport in a Pilot Scale Copper Electrowinning Cell, *J. Electrochem. Soc.* 163 (2016) E111-E122.

The authors perform detailed 3D finite-element simulations of the transport of  $\text{Cu}^{2+}$  by convection, diffusion and migration, and the transport of anode slime particles in a pilot-scale cell for copper electrowinning with an inlet at its bottom and an outlet at its top; the simulation results are compared with experimental data. A temperature gradient is imposed in the vertical direction; the dependences of viscosity, density and  $D_{\text{Cu}^{2+}}$  on  $T$  and concentration are all taken into account. The simulated velocity profiles show good agreement with the experimental, which are probed at a discrete set of points. The transport of slime particles in the solution is simulated and it is shown that the frequency of their appearance near the cathode correlates with the experimentally measured concentration of impurities in it.

43. \* W. Zeng, S. Wang, M.L. Free, A Comparative Study of Electrolyte Flow and Slime Particle Transport in a Newly Designed Copper Electrolytic Cell and a Laboratory-Scale Conventional Electrolytic Cell, *JOM* (2016), doi:10.1007/s11837-016-2076-x.

Simulations analogous to those in Ref. [42] are performed for a new cell with an inlet at the top and an outlet at the bottom and a conventional cell. It is shown that the former design reduces the likelihood of slime particles reaching the cathode and warrants a more uniform distribution of  $\text{Cu}^{2+}$  in the solution, thereby allowing the electrodeposition process to be run at higher current densities and lower  $\text{Cu}^{2+}$  concentrations.

44. W. Zeng, G. Yi, S. Wang, M.L. Free, Design and analysis of direct side inflows in copper electrolytic cells by a computational method, *Hydrometallurgy* 169 (2017) 612-620. Same as [42-43], different cell design.

45. M. Najmnoori, A. Mohebbi, B.G. Arabi, S. Daneshpajouh, CFD simulation of an industrial copper electrowinning cell, *Hydrometallurgy* 153 (2015) 88-97.

46. L.M.A. Monzon, J.M.D. Coey, Magnetic fields in electrochemistry: The Lorentz force. A mini-review. *Electrochem. Commun.* 42 (2014) 38-41.

47. L.M.A. Monzon, J.M.D. Coey, Magnetic fields in electrochemistry: The Kelvin force. A mini-review, *Electrochem. Commun.* 42 (2014) 42-45.
48. V.R. Rao, A.C. Hegde, Effect of Induced Magnetic Field on Electrocrystallization of Zn-Ni Alloy and Their Corrosion Study, *J. Mater. Eng. Perform.* 23 (2014) 2067-2074.
49. X. Yang, S.Mühlenhoff, P.A. Nikrityuk, K. Eckert, The initial transient of natural convection during copper electrolysis in the presence of an opposing Lorentz force: Current dependence, *Eur. Phys. J. Special Topics* 220 (2013), 303-312.
50. D. Koschichow, G. Mutschke, X. Yang, A. Bund, J. Fröhlich, Numerical Simulation of the Onset of Mass Transfer and Convection in Copper Electrolysis Subjected to a Magnetic Field, *Russ. J. Electrochem.* 48 (2012) 682-691.
51. D. Baczyzmalski, T. Weier, C.J. Kähler, C. Cierpka, Near-wall measurements of the bubble- and Lorentz-force-driven convection at gas-evolving electrodes, *Exp. Fluids* 56 (2015) 162.
52. D. Baczyzmalski, F. Karnbach, X. Yang, G. Mutschke, M. Uhlemann, K. Eckert, C. Cierpka, On the Electrolyte Convection around a Hydrogen Bubble Evolving at a Microelectrode under the Influence of a Magnetic Field, *J. Electrochem. Soc.* 163 (2016) E248-E257.
53. C.-K. Lim, B.-J. Chung, Influence of a center anode in analogy experiments of long flow ducts, *Int. Commun. Heat Mass Transf.* 56 (2014) 174-180.
54. J.-Y. Moon, B.-J. Chung, Time-dependent Rayleigh–Benard convection: Cell formation and Nusselt number, *Nucl. Eng. Des.* 274 (2014) 146-153.
55. J.-H. Heo, M.-S. Chae, B.-J. Chung, Influences of vertical and horizontal pitches on the natural convection of two staggered cylinders, *Int. J. Heat Mass Transfer* 57 (2013) 1-8.
56. H. Vogt, Single-Phase Free Convective Mass Transfer in Electrochemical Reactors, *Can. J. Chem. Eng.* 94 (2016) 368-373.
57. C. Amatore, S. Szunerits, L. Thouin, J.-S. Warkocz, The real meaning of Nernst's steady diffusion layer concept under non-forced hydrodynamic conditions. A simple model based on Levich's seminal view of convection, *J. Electroanal. Chem.* 500 (2001) 62-70.
58. A.S. Demeter, O. Dolgikh, A.C. Bastos, D. Deconinck, S. Lamaka, V. Topa, J. Deconinck, Multi-ion transport and reaction model used to improve the understanding of local current density measurements in presence of concentration gradients around a point current source, *Electrochim. Acta* 127 (2014) 45-52.
59. L.C. Abodi, Y. Gonzalez-Garcia, O. Dolgikh, C. Dan, D. Deconinck, J.M.C. Mol, H. Terryn, J. Deconinck, Simulated and measured response of oxygen SECM-measurements in presence of a corrosion process, *Electrochim. Acta* 146 (2014) 556-563.
60. C. Pebay, C. Sella, L. Thouin, C. Amatore, Mass Transport at Infinite Regular Arrays of Microband Electrodes Submitted to Natural Convection: Theory and Experiments, *Anal. Chem.* 85 (2013) 12062-12069.
61. O.V. Klymenko, I. Svir, C. Amatore, New theoretical insights into the competitive roles of electron transfers involving adsorbed and homogeneous phases, *J. Electroanal. Chem.* 688 (2013) 320-327.
62. O.V. Klymenko, I. Svir, C. Amatore, A New Approach for the Simulation of Electrochemiluminescence (ECL), *ChemPhysChem* 14 (2013) 2237-2250.
63. O. Dolgikh, A.S. Demeter, A.C. Bastos, V. Topa, J. Deconinck, A practical way to model convection in non-agitated electrolytes, *Electrochem. Commun.* 37 (2013) 20-23.
64. C. Amatore, C. Pebay, C. Sella, L. Thouin, Mass Transport at Microband Electrodes: Transient, Quasi-Steady-State, and Convective Regimes, *ChemPhysChem* 13 (2012) 1562-1568.
65. C. Amatore, O.V. Klymenko, I. Svir, Importance of Correct Prediction of Initial Concentrations in Voltammetric Scans: Contrasting Roles of Thermodynamics, Kinetics, and Natural Convection, *Anal. Chem.* 84 (2012) 2792-2798.
66. V.G. Levich, *Fiziko-khimicheskaya gidrodinamika*, Second edition, Gos. izd-vo fiziko-matematicheskoi lit-ry, Moscow, 1959.

67. K.-Q. Xia, C. Sun, S.-Q. Zhou, Particle image velocimetry measurement of the velocity field in turbulent thermal convection, *Phys. Rev. E* 68 (2003), 066303.
68. C. Amatore, S. Szunerits, L. Thouin, J.-S. Warkocz, Monitoring Concentration Profiles In Situ with an Ultramicroelectrode Probe, *Electroanalysis* 13 (2001) 646-652.
69. C. Amatore, C. Pebay, L. Thouin, A. Wang, J.-S. Warkocz, Difference between Ultramicroelectrodes and Microelectrodes: Influence of Natural Convection, *Anal. Chem.* 82 (2010) 6933-6939.
70. C. Amatore, C. Pebay, L. Thouin, A. Wang, Cyclic voltammetry at microelectrodes. Influence of natural convection on diffusion layers as characterized by in situ mapping of concentration profiles, *Electrochem. Commun.* 11 (2009) 1269-1272.
71. N. Baltes, L. Thouin, C. Amatore, J. Heinze, Imaging Concentration Profiles of Redox-Active Species with Nanometric Amperometric Probes: Effect of Natural Convection on Transport at Microdisk Electrodes, *Angew. Chem. Int. Ed.* 43 (2004) 1431-1435.
72. C. Amatore, K. Knobloch, L. Thouin, First direct experimental evidence of migration contributions through monitoring of concentration profiles at low supporting electrolyte concentration, *Electrochem. Commun.* 6 (2004) 887-891.
73. C. Amatore, K. Knobloch, L. Thouin, Alteration of diffusional transport by migration and natural convection. Theoretical and direct experimental evidences upon monitoring steady-state concentration profiles at planar electrodes, *J. Electroanal. Chem.* 601 (2007) 17-28.

## Graphical abstract

